

Moving Stone in the Hele-Shaw Flow

Gennady Mishuris¹, Sergei Rogosin^{1,2,*}, Michal Wrobel¹

¹*Aberystwyth University, Penlais, SY23 3BZ Aberystwyth, UK;*

e-mails: ggm@aber.ac.uk; ser14@aber.ac.uk; miw15@aber.ac.uk

²*Belarusian State University, Nezavisimosti Ave., 4, 220030 Minsk, Belarus;*

e-mail: rogosin@bsu.by

Abstract

Asymptotic analysis of the Hele-Shaw flow with a small moving obstacle is performed. The method of solution utilises the uniform asymptotic formulas for Green's and Neumann functions recently obtained by V. Maz'ya and A. Movchan. Theoretical results of the paper are illustrated by the numerical simulations.

Keywords: Hele-Shaw flow, moving obstacle, Green's function, Neumann function, asymptotic analysis

AMS 2010 Mathematics Subject Classification: 76D27, 35J25, 35R35

*Corresponding author.

1 Introduction

The paper is devoted to the asymptotic study of the flow in the Hele-Shaw cell with presence of moving obstacle in the flow.

The Hele-Shaw problem ([18]) deals with the description of the free boundary encircling the domain occupied by incompressible fluid in the so called Hele-Shaw cell (see, e.g. [16], [37]), i.e. in a narrow space between two parallel plates. Different driving mechanisms can be considered for the fluid flow, e.g. presence of a source/sink in the fluid domain.

Various physical assumptions lead to different formulations of the respective boundary value problems. A comprehensive discussion on this topic can be found in the recent book by Gustafsson and Vasil'ev [16].

There exist two basic mathematical models for the flow in the Hele-Shaw cell. The *complex-analytic model* is formulated as a nonlinear mixed boundary value problem with respect to a family of conformal mappings of the

canonical domain onto the domain occupied by the fluid. This approach goes back to the work by Polubarinova-Kochina [31] and Galin [11]. The proof of the existence (locally in time) and uniqueness of analytic solutions to this model was done by Kufarev & Vinogradov [21] (rediscovered later by Richardson [36]) on the basis of the method of successive approximations. Simplified proof of existence and uniqueness of an analytic solution was given by Reissig & von Wolfersdorf [33] (see also [32], [35]). In this work the model was interpreted as a special case of an abstract Cauchy-Kovalevsky problem, which was solved by a variant of the Cauchy-Kovalevsky theorem ([27], [28], [29]). See also [5] and references therein for the survey of recent results on the complex-analytic Hele-Shaw problem in doubly connected domains. Let us note that there are some similarities between movement of the rigid body and movement of bubbles in the flow (for the discussion of the latter process we refer, e.g., to the article [8] and references therein).

In our study we use the *real-variable model* proposed by Gustafsson [14] the flow is described by a family of parametrizations of the boundary of fluid domain (see also [19]). This model was generalized to multi-dimensional case by Begehr & Gilbert [4]. Among variants of the proof of existence and uniqueness for this model we have to point out the papers by Reissig [34] and by Escher & Simonett [10]. In the most general form, the proof of the existence, uniqueness of the classical solution and the regularity of the fluid boundary was given by Antontsev, Gonçalves and Meirmanov [1], [2].

Variational formulation of the Hele-Shaw model was proposed by Gustafsson [15], who proved the weak solvability of the problem (see also [3], [16]).

The classical (real-variable) Hele-Shaw model can be reinterpreted as a mixed boundary value problem for Laplace equation with respect to unknown parametrization of the boundary and corresponding Green's function of this problem in the reference domain. When assuming the presence of a moving obstacle in the flow, we have to add an additional equation describing this movement. The aim of our work is to perform an asymptotic analysis for such a variant of the model and to construct an efficient and robust numerical routine to tackle the problem.

Application of asymptotic methods to approximation of Green's function goes back to the classical paper by J. Hadamard [17], where the method of regular perturbation was performed. Recently, V. Maz'ya and A. Movchan obtained a number of asymptotic formulas for Green's function related to different boundary value problems for a number of differential operators in the case of singular perturbations of the domains (see [22], [23], [25] and

references therein).

Those results were used in [26] to model the Hele-Shaw flow with a fixed circular obstacle. To construct the computational scheme, we choose Green's formula with the Neumann condition on the external boundary of doubly connected domain, and with Dirichlet condition on its internal boundary. Then a preliminary transformation $\zeta = \varepsilon/z$ was made, which led to creation of a system of differential equations for the original problem approximation. The existence of the reformulated Hele-Shaw problem follows immediately from the results of the paper Escher-Simonett (1997b).

The approximate system defined in this way was reduced to the system of first order ODEs, and tackled by a proposed numerical scheme. This approach proved its ability to solve the analyzed Hele-Shaw problem, providing sufficiently good accuracy of computations.

However, the scheme itself exhibited some disadvantages:

- 1) in the case of sink the life-time of the approximate process was very short;
- 2) in the case of source we get numerical result only on a bounded interval of time.

The first difficulty could have been expected from the theory of the Hele-Shaw problem, but the second one is a consequence of the numerical scheme instability. In the case of moving obstacle this led to even worse results.

In this paper we consider the Hele-Shaw flow with a rigid inclusion moving in the direction of the flow without rotation. The friction between the limiting planes and the obstacle is accounted for. To avoid problems appeared in the case of the fixed obstacle, we use here the same Maz'ya-Movchan approach, but with different uniform asymptotic formula for Green's function (without making any preliminary transformations, and thus interchanging the role of boundary conditions).

The paper is organized as follows. Sec. 2 describes the problem's geometry and presents the (real-variable) Hele-Shaw model in a domain with a moving obstacle. The model is further reduced to the form containing an unknown parametrization of the boundary of the fluid domain, an unknown Green's function of the corresponding mixed boundary value problem for the Laplace operator and unknown trajectory of the inclusion. Therefore we have to consider a system of equations consisting of the equation for the free boundary (the standard Hele-Shaw equation) and the equation of motion for the obstacle. In Sec. 3 we present uniform asymptotic formula by Maz'ya-Movchan and describe its components. In Sec. 4 we determine the values of the components of the Maz'ya-Movchan formula correspond-

ing to the considered model. The final form of the approximate system of differential equations is presented in Subsec. 4.4. Finally, in Sec. 5 the aforementioned system is implemented in a numerical scheme which illustrates the obtained results. The numerical scheme to obtain the solution employs reduction of the system of governing equations to the system of ODEs of the first order, where the velocity of the inclusion is introduced as an additional dependent variable. In order to solve the dynamic system we utilize the standard ODE solver of Matlab package: ode45. Respective conformal mappings of the boundary curve are performed by means of the Schwartz-Christoffel Toolbox. The derivatives of the mapping along the free boundary are computed by our own subroutines, based on the spline approximation. We show that the used asymptotic expansion for the Green function is effective and the computations based on that approach are stable and robust.

2 Problem formulation

We consider the slow flow in the Hele-Shaw cell (i.e. in the narrow gap between two parallel plates of distance h). The flow is caused by a source/sink (situated at the origin $O = (0, 0)$) of intensity Q . The fluid of the viscosity μ occupies the bounded doubly connected domain $D_1(t)$ at the time instant $t \geq 0$ that takes the form $D_1(t) = D(t) \setminus F$, where $D(t)$ is a bounded simply-connected domain, and the compact set $F \subset D(t)$ is a small obstacle embedded within the fluid. The obstacle is moving in the direction of flow rotation free and with friction coefficient κ . To avoid technical difficulties, we accept a circular shape of the obstacle of the radius ε and of center $\mathbf{z}_0(t)$ at each instant of time t .

Suppose that our initial geometry satisfies the following conditions¹

$$c \leq \min \text{dist} \{O, D(0)\} \leq \max \text{dist} \{O, D(0)\} \leq 1,$$

$$\text{dist} \{\partial F, \partial D(0)\} = d > \varepsilon, \quad d + 2\varepsilon > c. \quad (2.1)$$

Following [2], the initial free boundary $\partial D(0)$ is to satisfy the smoothness assumptions

$$\partial D(0) \in \mathcal{C}^{2,\alpha}, \quad (2.2)$$

with certain fixed $\alpha, 0 < \alpha < 1$.

¹Note that both constants c and d do not depend on δ .

Omitting the standard description of the (real-variable) Hele-Shaw model (see, e.g. [16], [19], cf. [26]) we arrive at the following problem with respect to unknown parametrization $\mathbf{w}(s, t)$ of the free boundary $\Gamma(t) = \partial D(t)$ (i.e. the boundary value of the conformal mapping of the unit disc \mathbb{U} onto the fluid domain $D_1(t)$), Green's function $\mathcal{G}(\mathbf{z}; \zeta; t)$ of the domain $D_1(t)$ and the center $\mathbf{z}_0(t)$ of the obstacle.²

Problem (HS_{move}). Find a triple $\{\mathbf{w}(s, t) = (w_1(s, t), w_2(s, t)); \mathcal{G}(\mathbf{z}; \zeta; t); \mathbf{z}_0(t) = (z_{0,1}(t), z_{0,2}(t))\}$, satisfying the following conditions

- (i) $\mathbf{w}(s, t) \in \Gamma(t)$ for all $(s, t) \in \partial \mathbb{U} \times I$;
- (ii) $\mathbf{w}(\cdot, t) : \partial \mathbb{U} \rightarrow \Gamma(t)$ is a \mathcal{C}^2 -diffeomorphism for each fixed $t \in I$;
- (iii) $\mathbf{w}^{(0)}(s) = \mathbf{w}(s, 0)$ is a given \mathcal{C}^2 -diffeomorphism of the unit circle $\partial \mathbb{U}$, which describes the boundary $\Gamma(0)$ of initial domain $D_1(0)$;
- (iv) $\mathcal{G}(\mathbf{z}; \zeta; t)$ is Green's function of the operator $-\Delta$ in the doubly connected domain $D_1(t)$ with the homogeneous Neumann condition on ∂F and the homogeneous Dirichlet condition on $\Gamma(t)$;
- (v) $\partial_t \mathbf{w}(s, t) = -\frac{Qh^2}{12\mu} \cdot \nabla \mathcal{G}(\mathbf{w}(s, t); O; t)$ for all $(s, t) \in \partial \mathbb{U} \times I$;
- (vi) $\mathbf{z}_0'' + \frac{\kappa\pi\delta^2}{m} \mathbf{z}_0' = \frac{Q\delta}{m} \int_0^{2\pi} \mathcal{G}(z_{0,1} + \delta \cos \theta, z_{0,2} + \delta \sin \theta; O; t) \cdot \mathbf{n}^{(in)}(\theta) d\theta$,
- (vii) $\mathbf{z}_0(0) = \mathbf{z}^{(0)}$, $\mathbf{z}_0'(0) = \mathbf{z}^{(1)}$.

The aim of our study is to get an approximate solution to the problem **HS_{move}**.

3 Uniform representation of Green's function

In order to replace the system of equation (i)–(vii) of the Problem (**HS_{move}**) by the approximate system we use one the results by Maz'ya and Movchan. For further convenience, we introduce here a small parameter ε equal to the radius of the inclusion, and denote by $F_0 = F_0(t)$ the rescaled obstacle $F_0(t) = \{\mathbf{x} : \frac{1}{\varepsilon}(\mathbf{x} - \mathbf{z}_0(t)) \in F\}$. Note that for each $t \in I$ we have $F_0(t) = B(O; 1)$.

For the reader's convenience, we reformulate in our notation the theorem by V. Maz'ya and A. Movchan providing uniform asymptotic approximation

²Unknown magnitudes \mathbf{w} , \mathcal{G} , \mathbf{z}_0 depend on time t from a right-sided neighborhood I of $t = 0$. In fact, for our problem we need to determine the value of $\mathcal{G}(\mathbf{z}; \zeta; t)$ only at the point $\zeta = O$, but we keep the extra variable ζ for computational reasons.

of Green's function with the Neumann data on the boundary of the obstacle $F = B(\mathbf{z}_0, \varepsilon)$ and the Dirichlet data on the boundary of the domain D .

Theorem 3.1. [25, Thm. 2.1] *Let D_1 be a bounded doubly connected domain in \mathbb{R}^2 with a smooth boundary, $D_1 = D \setminus F$, where D is a simply connected domain and $F \subset D$ is a compact set (obstacle) with diameter smaller than the distance of ∂F to ∂D .*

Green's function $\mathcal{G}_\varepsilon(\mathbf{x}, \mathbf{y})$ of the Laplace operator $-\Delta$ with the Neumann zero-data on ∂F and the Dirichlet zero-data on ∂D has the following uniform asymptotic representation

$$\begin{aligned} \mathcal{G}_\varepsilon(\mathbf{x}, \mathbf{y}) = & G(\mathbf{x}, \mathbf{y}) + \mathcal{N} \left(\frac{1}{\varepsilon}(\mathbf{x} - \mathbf{z}_0), \frac{1}{\varepsilon}(\mathbf{y} - \mathbf{z}_0) \right) + \frac{1}{2\pi} \log \left| \frac{1}{\varepsilon}(\mathbf{x} - \mathbf{y}) \right| + \\ & + \varepsilon \mathcal{D} \left(\frac{1}{\varepsilon}(\mathbf{x} - \mathbf{z}_0) \right) \cdot \nabla_{\mathbf{x}} H(\mathbf{z}_0, \mathbf{y}) + \varepsilon \mathcal{D} \left(\frac{1}{\varepsilon}(\mathbf{y} - \mathbf{z}_0) \right) \cdot \nabla_{\mathbf{y}} H(\mathbf{x}, \mathbf{z}_0) + \mathbf{r}_\varepsilon(\mathbf{x}, \mathbf{y}), \end{aligned} \quad (3.1)$$

where $|\mathbf{r}_\varepsilon(\mathbf{x}, \mathbf{y})| \leq \text{Const} \cdot \varepsilon^2$.

In what follows we use this formula in the fluid domain $D_1(t)$ for all $t \in I = [0, T]$, for which the solution to the Hele-Shaw problem exists. In the case of the flow without obstacle or with a fixed obstacle we refer for the existence to [1]. In our case there is no rigorous proof of the existence, but it can be obtained similarly to that for the flow of bubbles (see, e.g. [8] and references therein).

In our case we accept in this Theorem the following notation for each instant of time $t \in I$. $G(\mathbf{x}, \mathbf{y}) = G(\mathbf{x}, \mathbf{y}; t)$ is Green's function of the Laplace operator $-\Delta$ for the simply connected domain $D = D(t)$ with zero Dirichlet data on $\partial D(t)$:

$$G(\mathbf{x}, \mathbf{y}) = \frac{1}{2\pi} \log \left| \frac{1}{\mathbf{x} - \mathbf{y}} \right| - H(\mathbf{x}, \mathbf{y}), \quad (3.2)$$

with H being the regular part of Green's function, i.e. harmonic function solving the following boundary value problem

$$\Delta_{\mathbf{x}} H(\mathbf{x}, \mathbf{y}) = 0, \quad \mathbf{x}, \mathbf{y} \in D(t), \quad (3.3)$$

$$H(\mathbf{x}, \mathbf{y}) = \frac{1}{2\pi} \log \left| \frac{1}{\mathbf{x} - \mathbf{y}} \right|, \quad \mathbf{x} \in \partial D(t), \mathbf{y} \in D(t). \quad (3.4)$$

$\mathcal{N}(\xi, \eta)$ is the Neumann function for the exterior of the re-scaled obstacle $F_0 = F_0(t)$:

$$\mathcal{N}(\xi, \eta) = \frac{1}{2\pi} \log |\xi - \eta|^{-1} - h_{\mathcal{N}}(\xi, \eta), \quad \xi, \eta \in \mathbb{R}^2 \setminus F_0(t), \quad (3.5)$$

where $h_{\mathcal{N}}(\xi, \eta)$ is the regular part of this function satisfying

$$\Delta_{\xi} h_{\mathcal{N}}(\xi, \eta) = 0, \quad \xi, \eta \in \mathbb{R}^2 \setminus F_0(t), \quad (3.6)$$

$$\frac{\partial h_{\mathcal{N}}(\xi, \eta)}{\partial n_{\xi}} = \frac{1}{2\pi} \frac{\partial}{\partial n_{\xi}} (\log |\xi - \eta|^{-1}), \quad \xi \in \partial F_0(t), \eta \in \mathbb{R}^2 \setminus F_0(t), \quad (3.7)$$

$$h_{\mathcal{N}}(\xi, \eta) \rightarrow 0, \quad |\xi| \rightarrow \infty, \eta \in \mathbb{R}^2 \setminus F_0(t). \quad (3.8)$$

The vector-function $\mathcal{D}(\xi) = (\mathcal{D}_1(\xi), \mathcal{D}_2(\xi))^T$ is the solution of the following boundary value problems in the exterior of the re-scaled obstacle $F_0 = F_0(t)$:

$$\Delta \mathcal{D}_j(\xi) = 0, \quad \xi \in \mathbb{R}^2 \setminus F_0(t), \quad j = 1, 2, \quad (3.9)$$

$$\frac{\partial \mathcal{D}_j(\xi)}{\partial n} = n_j, \quad \xi \in \partial F_0(t), \quad j = 1, 2, \quad (3.10)$$

$$\mathcal{D}_j(\xi) \rightarrow 0, \quad |\xi| \rightarrow \infty, \quad j = 1, 2. \quad (3.11)$$

Here n_j are components of the inward unit vector normal to the boundary of disc $F_0(t)$.

4 System of equations for the problem HS_{move}

4.1 Green's function $\mathcal{G}_{\varepsilon}$ for the problem HS_{move}

In this subsection we analyze the components of the representation (3.1). Let us first consider the Neumann function $\mathcal{N}(\xi, \eta)$ having in this case an explicit representation (see, e.g., [30, p. 68]):

$$\mathcal{N}(\xi, \eta) = -\frac{1}{4\pi} \log |\xi - \eta|^2 - \frac{1}{4\pi} \log \left[\frac{(|\xi|^2 - 1)(|\eta|^2 - 1) + |\xi - \eta|^2}{|\xi|^2 |\eta|^2} \right]. \quad (4.1)$$

satisfying the conditions (3.5), (3.6)–(3.8) and symmetric $\mathcal{N}(\xi, \eta) = \mathcal{N}(\eta, \xi)$. Its regular part $h_{\mathcal{N}}(\xi, \eta)$ is also symmetric and calculated explicitly yields

$$h_{\mathcal{N}}(\xi, \eta) = \frac{1}{4\pi} \log \left[\frac{(|\xi|^2 - 1)(|\eta|^2 - 1) + |\xi - \eta|^2}{|\xi|^2 |\eta|^2} \right]. \quad (4.2)$$

Green's function $G(\mathbf{x}; \mathbf{y}; t)$ for the interior simply connected domain $D(t)$ can be represented in the form

$$G(\mathbf{x}; \mathbf{y}; t) = -\frac{1}{2\pi} \log |g(\mathbf{x}, \mathbf{y})|, \quad (4.3)$$

where $g(\mathbf{x}, \mathbf{y}) = (g_1(\mathbf{x}, \mathbf{y}), g_2(\mathbf{x}, \mathbf{y})) : D(t) \rightarrow \mathbb{U}$ is the conformal mapping of $D(t)$ onto the unit disc \mathbb{U} , satisfying the following normalizing conditions $g(\mathbf{x}, \mathbf{y})|_{\mathbf{x}=\mathbf{y}} = 0$, and $g'(\mathbf{x}, \mathbf{y})|_{\mathbf{x}=\mathbf{y}} > 0$. In our case, $\mathbf{y} = O$ stands for the source/sink point (we again note that from computational point of view it is better to keep extra-variable \mathbf{y} up to the final formula). From the numerical point of view it is customary to start with an arbitrary conformal mapping $g_0(\mathbf{x}) : D(t) \rightarrow \mathbb{U}$ and determine the normalized one:

$$g(\mathbf{x}, \mathbf{y}) = \frac{g_0(\mathbf{x}) - g_0(\mathbf{y})}{1 - \overline{g_0(\mathbf{y})}g_0(\mathbf{x})}.$$

The vector-function $\mathcal{D}(\xi)$ can be found by using integral representation of the solution to the exterior Neumann problem for the unit disc (see, e.g., [30, p. 68]). First we note that the inward unit normal vector on the boundary of the unit disc $F_0(t)$ is

$$\mathbf{n}^{(in)} = \left(n_1^{(in)}, n_2^{(in)} \right) = -(\cos \varphi, \sin \varphi), \quad (4.4)$$

where φ is the angular coordinate of polar system on the unit circle $\partial F_0(t)$. Then the solutions to the problems (3.9)–(3.11) ($j = 1, 2$) are represented in the form

$$\mathcal{D}_j(\xi) = \frac{1}{2\pi} \int_0^{2\pi} \log \left(\frac{1}{r^2} + 1 - \frac{2}{r} \cos(\theta - \varphi) \right) n_j^{(in)} d\varphi, \quad j = 1, 2, \quad (4.5)$$

where $\xi = (r \cos \theta, r \sin \theta)$, $r > 1$. It is easy to see that the above functions satisfy all conditions (3.9)–(3.11). We calculate (4.5) using formula [13, (4.397.6)]:

$$\mathcal{D}_1(\xi) = \frac{1}{2} \frac{\xi_1}{\xi_1^2 + \xi_2^2}, \quad \mathcal{D}_2(\xi) = \frac{1}{2} \frac{\xi_2}{\xi_1^2 + \xi_2^2}. \quad (4.6)$$

4.2 Derivatives of Green's function

Here we calculate derivatives of Green's function which are used in equation (v) of the Problem (**HS_{move}**). We start with Green's function $G(\mathbf{x}; \mathbf{y}) = G(\mathbf{x}; \mathbf{y}; t)$. By applying representation (4.3) we have ($j = 1, 2$)

$$\partial_{x_j} G(\mathbf{x}; \mathbf{y}) = -\frac{1}{2\pi} \frac{g_1(\mathbf{x}; \mathbf{y}) \partial_{x_j} g_1(\mathbf{x}; \mathbf{y}) + g_2(\mathbf{x}; \mathbf{y}) \partial_{x_j} g_2(\mathbf{x}; \mathbf{y})}{g_1^2(\mathbf{x}; \mathbf{y}) + g_2^2(\mathbf{x}; \mathbf{y})}. \quad (4.7)$$

Substituting $\mathbf{x} = (w_1(s, t), w_2(s, t))$, $\mathbf{y} = (0, 0)$ and taking into account the properties of the function $g(\mathbf{x}; \mathbf{y})$ we finally obtain

$$\begin{aligned} \partial_{x_j} G(w_1(s, t), w_2(s, t); 0, 0) = \\ = -\frac{1}{2\pi} (g_1(w_1(s, t), w_2(s, t); 0, 0) \partial_{w_j} g_1(w_1(s, t), w_2(s, t); 0, 0) + \\ + g_2(w_1(s, t), w_2(s, t); 0, 0) \partial_{w_j} g_2(w_1(s, t), w_2(s, t); 0, 0)). \end{aligned} \quad (4.8)$$

The Neumann function $\mathcal{N}(\xi; \eta)$ depends on the ‘‘scaled’’ variables

$$\xi = \frac{1}{\varepsilon} (\mathbf{x} - \mathbf{z}_0(t)), \quad \eta = \frac{1}{\varepsilon} (\mathbf{y} - \mathbf{z}_0(t)). \quad (4.9)$$

Hence

$$\partial_{x_j} \mathcal{N}(\xi; \eta) = \partial_{\xi_j} \mathcal{N}(\xi; \eta) \frac{\partial \xi_j}{\partial x_j} = \frac{1}{\varepsilon} \partial_{\xi_j} \mathcal{N}(\xi; \eta).$$

Using explicit representation of the Neumann function (4.1) we get the following value of the derivatives ($j = 1, 2$)

$$\begin{aligned} \partial_{x_j} \mathcal{N}(\xi; \eta) = -\frac{1}{2\pi\varepsilon} \frac{\xi_j - \eta_j}{(\xi_1 - \eta_1)^2 + (\xi_2 - \eta_2)^2} + \frac{1}{2\pi\varepsilon} \frac{\xi_j}{\xi_1^2 + \xi_2^2} - \\ - \frac{1}{2\pi\varepsilon} \left[\frac{\xi_j(\eta_1^2 + \eta_2^2) - \eta_j}{(\xi_1^2 + \xi_2^2 - 1)(\eta_1^2 + \eta_2^2 - 1) + (\xi_1 - \eta_1)^2 + (\xi_2 - \eta_2)^2} \right]. \end{aligned} \quad (4.10)$$

Now substitute $\xi_j = \frac{1}{\varepsilon} (w_j(s, t) - z_{0,j}(t))$, $\eta_j = -\frac{1}{\varepsilon} z_{0,j}(t)$, $j = 1, 2$ (in order to simplify representation we omit internal variables s and t in the right hand-side of this relation) and calculate derivatives of two terms of Maz'ya-Movchan asymptotic formula (see (3.1)) at $\mathbf{x} = (w_1, w_2)$ with $\mathbf{y} = (0, 0)$

$$\frac{\partial}{\partial x_j} \left(\mathcal{N}(\xi, \eta) + \frac{1}{4\pi} \log \left| \frac{1}{\varepsilon} (\mathbf{x} - \mathbf{y}) \right|^2 \right).$$

These derivatives (denoted K_j) are equal

$$\begin{aligned}
K_j &= \frac{\partial}{\partial x_j} \left(\mathcal{N}(\xi, \eta) + \frac{1}{4\pi} \log \left| \frac{1}{\varepsilon} (\mathbf{x} - \mathbf{y}) \right|^2 \right) = \quad (4.11) \\
&= -\frac{1}{2\pi} \left\{ \frac{(w_j - z_{0,j})[z_{0,1}^2 + z_{0,2}^2 - \varepsilon^2] + \varepsilon^2 w_j}{[(w_1 - z_{0,1})^2 + (w_2 - z_{0,2})^2 - \varepsilon^2][z_{0,1}^2 + z_{0,2}^2 - \varepsilon^2] + \varepsilon^2(w_1^2 + w_2^2)} \right. \\
&\quad \left. - \frac{w_j - z_{0,j}}{(w_1 - z_{0,1})^2 + (w_2 - z_{0,2})^2} \right\}.
\end{aligned}$$

Thus for $\varepsilon = 0$ we have $K_j = 0$.

For regular part $H(\mathbf{x}; \mathbf{y})$ of Green's function $G(\mathbf{x}; \mathbf{y})$ we have the representation (3.2), i.e.

$$H(\mathbf{x}; \mathbf{y}) = \frac{1}{2\pi} \log \left| \frac{g(\mathbf{x}; \mathbf{y})}{\mathbf{x} - \mathbf{y}} \right|.$$

Therefore

$$\begin{aligned}
\partial_{x_j} H(\mathbf{w}; O) &= +\frac{1}{2\pi} \frac{g_1(\mathbf{z}_0; O) \partial_{z_{0,j}} g_1(\mathbf{z}_0; O) + g_2(\mathbf{z}_0; O) \partial_{z_{0,j}} g_2(\mathbf{z}_0; O)}{g_1^2(\mathbf{z}_0; O) + g_2^2(\mathbf{z}_0; O)} - \quad (4.12) \\
&\quad - \frac{1}{2\pi} \frac{z_{0,j}}{z_{0,1}^2 + z_{0,2}^2} = \\
&= \frac{1}{2\pi} \left(g_1(\mathbf{w}; O) \partial_{w_j} g_1(\mathbf{w}; O) + g_2(\mathbf{w}; O) \partial_{w_j} g_2(\mathbf{w}; O) - \frac{w_j}{w_1^2 + w_2^2} \right).
\end{aligned}$$

Analogously,

$$\begin{aligned}
\partial_{y_j} H(\mathbf{x}; \mathbf{z}_0) &= +\frac{1}{2\pi} \frac{g_1(\mathbf{x}; \mathbf{z}_0) \partial_{y_j} g_1(\mathbf{x}; \mathbf{z}_0) + g_2(\mathbf{x}; \mathbf{z}_0) \partial_{y_j} g_2(\mathbf{x}; \mathbf{z}_0)}{g_1^2(\mathbf{x}; \mathbf{z}_0) + g_2^2(\mathbf{x}; \mathbf{z}_0)} + \quad (4.13) \\
&\quad + \frac{1}{2\pi} \frac{x_j - z_{0,j}}{(x_1 - z_{0,1})^2 + (x_2 - z_{0,2})^2}.
\end{aligned}$$

In this case the right hand-side of the last relation does depend on \mathbf{x} .

Now we have to calculate the derivatives with respect to \mathbf{x} of the following expression

$$J_1(\mathbf{x}, \mathbf{y}) := J_1 = \varepsilon \mathcal{D} \left(\frac{1}{\varepsilon} (\mathbf{x} - \mathbf{z}_0) \right) \cdot \nabla_{\mathbf{x}} H(\mathbf{z}_0; \mathbf{y}) =$$

$$= \varepsilon \mathcal{D}_1 \left(\frac{1}{\varepsilon} (\mathbf{x} - \mathbf{z}_0) \right) \partial_{x_1} H(\mathbf{z}_0; \mathbf{y}) + \varepsilon \mathcal{D}_2 \left(\frac{1}{\varepsilon} (\mathbf{x} - \mathbf{z}_0) \right) \partial_{x_2} H(\mathbf{z}_0; \mathbf{y}),$$

where only first multiplier in each summand depends on \mathbf{x} . Derivatives of \mathcal{D}_k in x_j is connected with that in ξ_j

$$\partial_{x_j} \left(\varepsilon \mathcal{D}_k \left(\frac{1}{\varepsilon} (\mathbf{x} - \mathbf{z}_0) \right) \right) = (\mathcal{D}_k)'_{\xi_j} \left(\frac{1}{\varepsilon} (\mathbf{x} - \mathbf{z}_0) \right), \quad j, k = 1, 2.$$

By the direct calculation we have

$$\begin{aligned} \partial_{x_1} J_1(\mathbf{w}, O) &= \frac{\varepsilon^2}{2} \left(\frac{(w_2 - z_{0,2})^2 - (w_1 - z_{0,1})^2}{((w_1 - z_{0,1})^2 + (w_2 - z_{0,2})^2)^2} \cdot \partial_{x_1} H(\mathbf{z}_0; O) - \right. \\ &\quad \left. - \frac{2(w_1 - z_{0,1})(w_2 - z_{0,2})}{((w_1 - z_{0,1})^2 + (w_2 - z_{0,2})^2)^2} \cdot \partial_{x_2} H(\mathbf{z}_0; O) \right), \end{aligned} \quad (4.14)$$

and

$$\begin{aligned} \partial_{x_2} J_1(\mathbf{w}, O) &= \frac{\varepsilon^2}{2} \left(-\frac{2(w_1 - z_{0,1})(w_2 - z_{0,2})}{((w_1 - z_{0,1})^2 + (w_2 - z_{0,2})^2)^2} \cdot \partial_{x_1} H(\mathbf{z}_0; O) - \right. \\ &\quad \left. - \frac{(w_2 - z_{0,2})^2 - (w_1 - z_{0,1})^2}{((w_1 - z_{0,1})^2 + (w_2 - z_{0,2})^2)^2} \cdot \partial_{x_2} H(\mathbf{z}_0; O) \right), \end{aligned} \quad (4.15)$$

where the derivatives $\partial_{x_j} H(\mathbf{z}_0; \mathbf{y})$ are presented in (4.12).

At last we have

$$\begin{aligned} J_2(\mathbf{x}, \mathbf{y}) &= J_2 = \varepsilon \mathcal{D} \left(\frac{1}{\varepsilon} (\mathbf{y} - \mathbf{z}_0) \right) \cdot \nabla_{\mathbf{y}} H(\mathbf{x}; \mathbf{z}_0) = \\ &= \varepsilon \mathcal{D}_1 \left(\frac{1}{\varepsilon} (\mathbf{y} - \mathbf{z}_0) \right) F_1(\mathbf{x}; \mathbf{z}_0) + \varepsilon \mathcal{D}_2 \left(\frac{1}{\varepsilon} (\mathbf{y} - \mathbf{z}_0) \right) F_2(\mathbf{x}; \mathbf{z}_0). \end{aligned}$$

Here, only second multiplier in each summand depends on \mathbf{x} , and

$$F_i = \partial_{y_i} H(\mathbf{x}; \mathbf{z}_0) = \frac{1}{2\pi} \partial_{y_i} \log \left| \frac{g(\mathbf{x}; \mathbf{y})}{\mathbf{x} - \mathbf{y}} \right|_{\mathbf{y}=\mathbf{z}_0}, \quad i = 1, 2.$$

Hence

$$\partial_{x_j} J_2 = \frac{\varepsilon}{2} \frac{\eta_1}{\eta_1^2 + \eta_2^2} \partial_{x_j} F_1 + \frac{\varepsilon}{2} \frac{\eta_2}{\eta_1^2 + \eta_2^2} \partial_{x_j} F_2, \quad j = 1, 2.$$

Therefore, since $\eta_i = -\frac{1}{\varepsilon} z_{0,i}$, $i = 1, 2$, and using (4.6) we have

$$\begin{aligned} \partial_{x_j} J_2(\mathbf{w}, O) &= -\frac{\varepsilon^2}{2} \frac{z_{0,1}}{z_{0,1}^2 + z_{0,1}^2} \cdot \partial_{x_j} F_1(\mathbf{w}; \mathbf{z}_0) - \frac{\varepsilon^2}{2} \frac{z_{0,2}}{z_{0,1}^2 + z_{0,1}^2} \cdot \partial_{x_j} F_2(\mathbf{w}; \mathbf{z}_0). \end{aligned} \quad (4.16)$$

4.3 Integrals of Green's function

In this subsection we calculate integrals from the right hand-side of the equation (vi) in the representation of **Problem (HS_{move})**:

$$P_j = \frac{Q\varepsilon}{m} \int_0^{2\pi} \mathcal{G}(\mathbf{x}; \mathbf{y}; t) n_j^{(in)}(\theta) d\theta, \quad j = 1, 2, \quad (4.17)$$

were $\mathbf{x} = (z_{0,1} + \varepsilon \cos \theta, z_{0,2} + \varepsilon \sin \theta)$, $\mathbf{y} = (0, 0)$.

In our calculations we use components of formula (3.1) and their representations obtained in Subsec. 4.1. First we calculate the integral

$$I_{1,1} := \int_0^{2\pi} G(\mathbf{x}; \mathbf{y}; t) \cos \theta d\theta |_{\mathbf{y}=O} \quad (4.18)$$

employing representation (4.3):

$$I_{1,1} = -\frac{1}{2\pi} \int_0^{2\pi} \log |g(\mathbf{x}; O)| \cos \theta d\theta = -\frac{1}{2\pi} \operatorname{Re} \int_0^{2\pi} \log g(\mathbf{x}; O) \cos \theta d\theta.$$

Note that for each fixed $t \in I$ the function $\log g(\mathbf{x}; O)$ is an analytic function with respect to variable $\mathbf{x} = (x_1, x_2)$ in the disc $B(\mathbf{z}_0, \varepsilon)$. Hence using Taylor expansion of $\log g(\mathbf{x}; O)$ at $\mathbf{x} = \mathbf{z}_0$ we have

$$I_{1,1} = -\frac{\varepsilon}{2} \operatorname{Re} c_1 + O(\varepsilon^3) = -\frac{\varepsilon}{2} \operatorname{Re} \frac{g'(\mathbf{z}_0, O)}{g(\mathbf{z}_0, O)} + O(\varepsilon^3). \quad (4.19)$$

Similar calculations can be performed for the integral

$$\tilde{I}_{1,1} := \int_0^{2\pi} G(\mathbf{x}; \mathbf{y}; t) \sin \theta d\theta |_{\mathbf{y}=O} = -\frac{\varepsilon}{2} \operatorname{Re} i c_1 + O(\varepsilon^3) = -\frac{\varepsilon}{2} \operatorname{Re} \frac{ig'(\mathbf{z}_0, O)}{g(\mathbf{z}_0, O)} + O(\varepsilon^3). \quad (4.20)$$

In the integral

$$I_{1,2} := \int_0^{2\pi} \left[\mathcal{N} \left(\frac{1}{\varepsilon} (\mathbf{x} - \mathbf{z}_0, \mathbf{y} - \mathbf{z}_0) \right) + \frac{1}{2\pi} \log \left| \frac{1}{\varepsilon} (\mathbf{x} - \mathbf{y}) \right| \right] \cos \theta d\theta |_{\mathbf{y}=O}, \quad (4.21)$$

we use representation (4.1)

$$\begin{aligned}
I_{1,2} &:= \int_0^{2\pi} \left[\mathcal{N} \left(\frac{1}{\varepsilon}(\mathbf{x} - \mathbf{z}_0, -\mathbf{z}_0) \right) + \frac{1}{2\pi} \log \left| \frac{\mathbf{x}}{\varepsilon} \right| \right] \cos \theta d\theta = \quad (4.22) \\
&= -\frac{1}{4\pi} \int_0^{2\pi} \log \left\{ \left(\frac{|\mathbf{x} - \mathbf{z}_0|^2}{\varepsilon^2} - 1 \right) \left(\frac{|\mathbf{z}_0|^2}{\varepsilon^2} - 1 \right) + \frac{|\mathbf{x}|^2}{\varepsilon^2} \right\} \cos \theta d\theta + \\
&\quad + \frac{1}{4\pi} \int_0^{2\pi} \log \left(\frac{|\mathbf{x} - \mathbf{z}_0|^2 |\mathbf{z}_0|^2}{\varepsilon^4} \right) \cos \theta d\theta.
\end{aligned}$$

Since $|\mathbf{x} - \mathbf{z}_0| = \varepsilon$ and $\int_0^{2\pi} C \cdot \cos \theta d\theta = 0$, then we have

$$I_{1,2} = -\frac{1}{2\pi} \int_0^{2\pi} \log |\mathbf{x}| \cos \theta d\theta = -\frac{1}{2\pi} \operatorname{Re} \int_0^{2\pi} \log \mathbf{x} \cos \theta d\theta.$$

The function $\log \mathbf{x}$ is an analytic function with respect to variable $\mathbf{x} = (x_1, x_2)$ in the disc $B(\mathbf{z}_0, \varepsilon)$. Hence

$$I_{1,2} = -\frac{\varepsilon}{2} \operatorname{Re} \frac{1}{\mathbf{z}_0} + O(\varepsilon^3). \quad (4.23)$$

Analogously for the integral $\tilde{I}_{1,2}$ we have

$$\begin{aligned}
\tilde{I}_{1,2} &:= \int_0^{2\pi} \left[\mathcal{N} \left(\frac{1}{\varepsilon}(\mathbf{x} - \mathbf{z}_0, \mathbf{y} - \mathbf{z}_0) \right) + \frac{1}{2\pi} \log \left| \frac{1}{\varepsilon}(\mathbf{x} - \mathbf{y}) \right| \right] \sin \theta d\theta \Big|_{\mathbf{y}=\mathbf{0}} = \quad (4.24) \\
&= -\frac{1}{2\pi} \int_0^{2\pi} \log |\mathbf{x}| \sin \theta d\theta = -\frac{1}{2\pi} \operatorname{Re} \int_0^{2\pi} \log \mathbf{x} \sin \theta d\theta = -\frac{\varepsilon}{2} \operatorname{Re} \frac{i}{\mathbf{z}_0} + O(\varepsilon^3).
\end{aligned}$$

Next we calculate

$$I_{1,3} := \int_0^{2\pi} \varepsilon \mathcal{D} \left(\frac{1}{\varepsilon}(\mathbf{x} - \mathbf{z}_0) \right) \cdot \nabla_{\mathbf{x}} H(\mathbf{z}_0; \mathbf{y}) \cos \theta d\theta. \quad (4.25)$$

Taking into account exact values (4.6) of the functions $\mathcal{D}_1(\xi)$, $\mathcal{D}_2(\xi)$ and parametrization of the boundary of $B(0; 1)$ ($\xi_1 = \cos \theta$, $\xi_2 = \sin \theta$) we obtain

$$I_{1,3} = \frac{\varepsilon}{2} \partial_{x_1} H(\mathbf{z}_0; \mathbf{y}) \int_0^{2\pi} \cos^2 \theta d\theta + \frac{\varepsilon}{2} \partial_{x_2} H(\mathbf{z}_0; \mathbf{y}) \int_0^{2\pi} \sin \theta \cos \theta d\theta = \frac{\pi\varepsilon}{2} \partial_{x_1} H(\mathbf{z}_0; \mathbf{y}).$$

Finally, using (4.12)

$$I_{1,3} = \frac{\varepsilon}{4} \left(\frac{g_1(\mathbf{z}_0; O) \partial_{x_1} g_1(\mathbf{z}_0; O) + g_2(\mathbf{z}_0; O) \partial_{x_1} g_2(\mathbf{z}_0; O)}{g_1^2(\mathbf{z}_0; O) + g_2^2(\mathbf{z}_0; O)} - \frac{z_{0,1}}{z_{0,1}^2 + z_{0,2}^2} \right). \quad (4.26)$$

Similar calculations lead

$$\tilde{I}_{1,3} := \int_0^{2\pi} \varepsilon \mathcal{D} \left(\frac{1}{\varepsilon} (\mathbf{x} - \mathbf{z}_0) \right) \cdot \nabla_{\mathbf{x}} H(\mathbf{z}_0; \mathbf{y}) \sin \theta d\theta = \frac{\pi\varepsilon}{2} \partial_{x_2} H(\mathbf{z}_0; \mathbf{y}), \quad (4.27)$$

$$\tilde{I}_{1,3} = \frac{\varepsilon}{4} \left(\frac{g_1(\mathbf{z}_0; O) \partial_{x_2} g_1(\mathbf{z}_0; O) + g_2(\mathbf{z}_0; O) \partial_{x_2} g_2(\mathbf{z}_0; O)}{g_1^2(\mathbf{z}_0; O) + g_2^2(\mathbf{z}_0; O)} - \frac{z_{0,2}}{z_{0,1}^2 + z_{0,2}^2} \right). \quad (4.28)$$

The last integral from (4.17) is calculated by using (4.6)

$$\begin{aligned} I_{1,4} &:= \int_0^{2\pi} \varepsilon \mathcal{D} \left(\frac{1}{\varepsilon} (\mathbf{y} - \mathbf{z}_0) \right) \cdot \nabla_{\mathbf{y}} H(\mathbf{x}; \mathbf{z}_0) \cos \theta d\theta = \quad (4.29) \\ &= -\frac{\varepsilon^2}{2(z_{0,1}^2 + z_{0,2}^2)} \int_0^{2\pi} [z_{0,1} \partial_{y_1} H(\mathbf{x}; \mathbf{z}_0) + z_{0,2} \partial_{y_2} H(\mathbf{x}; \mathbf{z}_0)] \cos \theta d\theta. \end{aligned}$$

Since $\log \frac{g(\mathbf{x}; \mathbf{z}_0)}{\mathbf{x} - \mathbf{z}_0}$ is an analytic function with respect to variable $\mathbf{x} = (x_1, x_2)$ in the disc $B(\mathbf{z}_0, \varepsilon)$ then

$$-\frac{Q\varepsilon}{m} I_{1,4} = O(\varepsilon^4).$$

Similar result we have for the integral

$$\tilde{I}_{1,4} := \int_0^{2\pi} \varepsilon \mathcal{D} \left(\frac{1}{\varepsilon} (\mathbf{y} - \mathbf{z}_0) \right) \cdot \nabla_{\mathbf{y}} H(\mathbf{x}; \mathbf{z}_0) \sin \theta d\theta, \quad (4.30)$$

$$-\frac{Q\varepsilon}{m}\tilde{I}_{1,4} = O(\varepsilon^4).$$

Note that

$$\begin{aligned} \operatorname{Re} \frac{g'(\mathbf{z}_0, O)}{g(\mathbf{z}_0, O)} &= \frac{g_1(\mathbf{z}_0; O)\partial_{x_1}g_1(\mathbf{z}_0; O) + g_2(\mathbf{z}_0; O)\partial_{x_1}g_2(\mathbf{z}_0; O)}{g_1^2(\mathbf{z}_0; O) + g_2^2(\mathbf{z}_0; O)}, \\ \operatorname{Re} i \frac{g'(\mathbf{z}_0, O)}{g(\mathbf{z}_0, O)} &= \frac{g_1(\mathbf{z}_0; O)\partial_{x_2}g_1(\mathbf{z}_0; O) + g_2(\mathbf{z}_0; O)\partial_{x_2}g_2(\mathbf{z}_0; O)}{g_1^2(\mathbf{z}_0; O) + g_2^2(\mathbf{z}_0; O)}, \\ \operatorname{Re} \frac{1}{\mathbf{z}_0} &= \frac{z_{0,1}}{z_{0,1}^2 + z_{0,2}^2}, \quad \operatorname{Re} \frac{i}{\mathbf{z}_0} = \frac{z_{0,2}}{z_{0,1}^2 + z_{0,2}^2}. \end{aligned}$$

Therefore, combining all above calculations we have

$$-\frac{Q\varepsilon}{m}[I_{1,1} + I_{1,2} + I_{1,3} + I_{1,4}] = \frac{Q\varepsilon^2}{4m}I + O(\varepsilon^4), \quad (4.31)$$

$$-\frac{Q\varepsilon}{m}[\tilde{I}_{1,1} + \tilde{I}_{1,2} + \tilde{I}_{1,3} + \tilde{I}_{1,4}] = \frac{Q\varepsilon^2}{4m}\tilde{I} + O(\varepsilon^4), \quad (4.32)$$

$$\begin{aligned} I &= \frac{g_1(\mathbf{z}_0; O)\partial_{x_1}g_1(\mathbf{z}_0; O) + g_2(\mathbf{z}_0; O)\partial_{x_1}g_2(\mathbf{z}_0; O)}{g_1^2(\mathbf{z}_0; O) + g_2^2(\mathbf{z}_0; O)} + 3\frac{z_{0,1}}{z_{0,1}^2 + z_{0,2}^2}, \\ \tilde{I} &= \frac{g_1(\mathbf{z}_0; O)\partial_{x_2}g_1(\mathbf{z}_0; O) + g_2(\mathbf{z}_0; O)\partial_{x_2}g_2(\mathbf{z}_0; O)}{g_1^2(\mathbf{z}_0; O) + g_2^2(\mathbf{z}_0; O)} + 3\frac{z_{0,2}}{z_{0,1}^2 + z_{0,2}^2}. \end{aligned}$$

4.4 Final system of differential equations

It follows from the potential theory (see, e.g. [12, Ch. 8], cf. [25, Lemma 2.3]), that for any compact subset $\Omega, \bar{\Omega} \subset D_1(t)$,

$$\left| (r_\varepsilon(\mathbf{x}, \mathbf{y}))'_{x_j} \right| \leq \varepsilon^3, \quad j = 1, 2, \quad \mathbf{x}, \mathbf{y} \in \bar{\Omega}.$$

Thus, the **Problem (HS_{move})** can be asymptotically approximated by the following system

$$\partial_t w_1 = -\frac{Qh^2}{12\mu} (\partial_{x_1} G(\mathbf{w}; O) + K_1 + \partial_{x_1} J_1(\mathbf{w}; O) + \partial_{x_1} J_2(\mathbf{w}; O)), \quad (4.33)$$

$$\partial_t w_2 = -\frac{Qh^2}{12\mu} (\partial_{x_2} G(\mathbf{w}; O) + K_2 + \partial_{x_2} J_1(\mathbf{w}; O) + \partial_{x_2} J_2(\mathbf{w}; O)), \quad (4.34)$$

$$z''_{0,1} + \frac{\kappa\pi\varepsilon^2}{m}z'_{0,1} = \frac{Q\varepsilon^2}{4m}I, \quad (4.35)$$

$$z''_{0,2} + \frac{\kappa\pi\varepsilon^2}{m}z'_{0,2} = \frac{Q\varepsilon^2}{4m}\tilde{I}, \quad (4.36)$$

with initial conditions $\mathbf{z}_0(0) = \mathbf{z}^{(0)}$, $\mathbf{z}'_0(0) = \mathbf{z}^{(1)}$. Here $\mathbf{w} = (w_1(s, t), w_2(s, t))$ is an unknown parametrization of the external boundary $\partial D(t)$, $\mathbf{z}_0 = (z_{0,1}(t), z_{0,2}(t))$ is an unknown position of the center of the moving obstacle and K_j , $\partial_{x_j}J_k$, I , \tilde{I} are defined in (4.11), (4.14), (4.15), (4.16), (4.31), (4.32).

5 Numerical examples and discussions

In this section we provide only a short illustration of efficiency of the proposed methods for applications.

The numerical scheme to obtain the solution employs reduction of the system of governing equations (4.33)-(4.34) to the system of ODEs of the first order, where the velocity of the inclusion is introduced as an additional dependent variable. In order to solve the dynamic system of the first order derived in this way we utilize the standard ODE solver of Matlab package: ode45. It is based on an explicit Runge-Kutta formula. Respective conformal mappings of the boundary curve are performed by means of the Schwartz-Christoffel Toolbox [6], [7]. The derivatives of the mapping along the free boundary are computed by our own subroutines, based on the spline approximation.

To investigate the accuracy of the proposed numerical scheme we use the classical benchmark by Polubarinova-Kochina [16, p. 29], which describes the fluid domain induced by a source or a sink without inclusion ($\varepsilon = 0$). Evolution of the free boundary in the considered case is illustrated in Fig.1. We analyze three different densities of the spatial meshing, described by the number of the nodes, N , distributed at uniform angular distances: $N = 35$, $N = 70$, $N = 120$. Moreover, both the fluid source and fluid sink variants are considered. In the first case the free boundary evolves from the internal to external shape (see Fig.1). In the second one it moves in reverse direction. The results of computations illustrated by the relative error of the radius vector defining the free boundary, $\delta\rho$, are shown in Fig.2.

It shows that the solution accuracy is of one order of magnitude better for the expansion ($\delta\rho = 10^{-6}$) than that for the contraction ($\delta\rho = 10^{-5}$) of

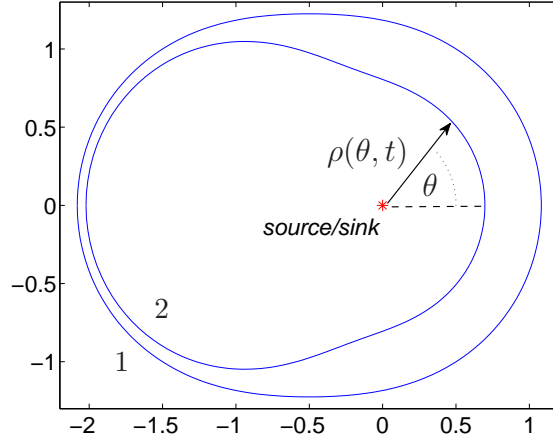


Figure 1: Evolution of the computational domain in time - the limiting curves. Both cases, contraction from the curve 1 to the curve 2 in case of the sink and expansion over the same time (from the curve 2 to the curve 1 in case of the source), are considered. Vector $\rho(\theta, t)$ defines the boundary curve.

the domain. Thus, the proposed algorithm is capable of tackling both cases with a satisfactory solution accuracy.

In the next step we investigate to what degree the presence of an immobile inclusion inside the domain affects the fluid flow. Now, we restrict ourselves only to the case of fluid source and consider a circular inclusion of the radius $\varepsilon = 0.2$ inside the domain encircled by the internal curve 2 from the previous benchmark. We retain the same source intensity and time interval assuming zero initial conditions ($\mathbf{z}^{(0)} = \mathbf{z}^{(1)} = 0$) in the absence of any forces in the right-hand sides of (4.35) - (4.36). Two various locations of the inclusion are considered: $\mathbf{z}_0 = 0.2 + 0.5i$ and $\mathbf{z}_0 = -1.55 - 0.55i$. The graphical illustration of the problem is shown in Fig. 3, where the final shapes for the free boundary for both variants are compared with the case of undisturbed flow depicted with markers.

Relative deviations of the radius vector, $\delta\rho$, from the one obtained for the undisturbed flow are shown in Fig. 4. As can be expected, the maximal distortion of the boundary curve takes place approximately along the direc-

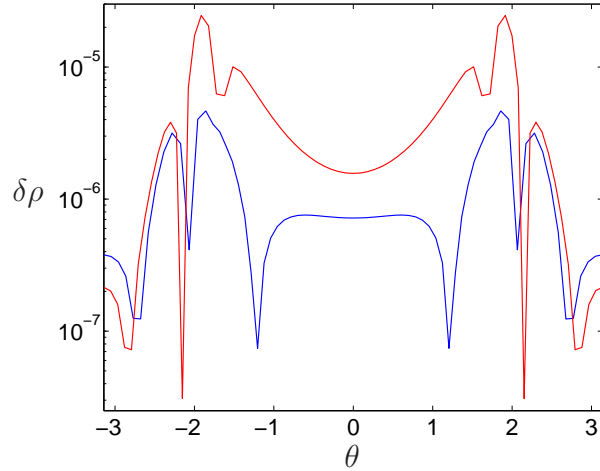


Figure 2: Relative error of the radius vector $\rho(t_{max}, \theta)$. Blue line corresponds the source case, while the red one refers to the sink configuration.

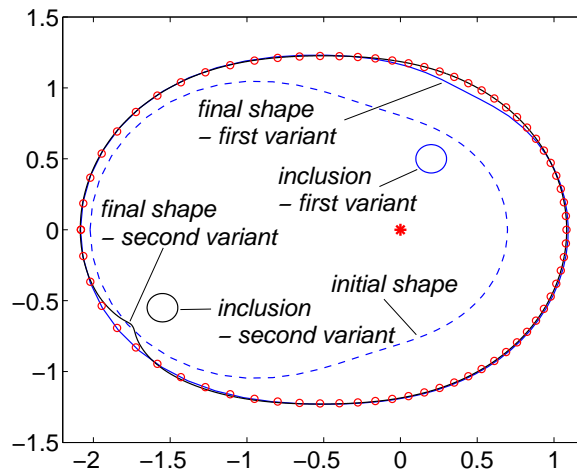


Figure 3: Graphical illustration of the problem with an immobile inclusion. Two locations of the obstacle are considered. The curve with markers corresponds to the results for undisturbed flow (without inclusion).

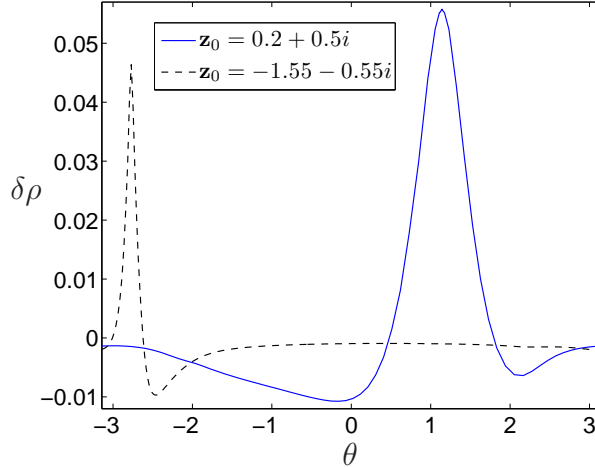


Figure 4: Relative deviation of the radius-vector for both variants of inclusion's location from Fig. 3. The reference value of ρ corresponds to the undisturbed flow.

tion source-inclusion. Moreover, the shorter the distance between the source and inclusion is, the more pronounced deviation from the reference value is obtained. Since in both cases the source supplies the same volume of fluid in the considered time, one can check the accuracy of computations in terms of the fluid balance. The respective areas are:

$$A = \frac{1}{2} \int_{-\pi}^{\pi} \rho^2(t_{max}, \theta) d\theta.$$

The relative deviations of A from the benchmark value were: $1.64 \cdot 10^{-6}$ and $4.51 \cdot 10^{-5}$ for the first and second location of the obstacle, respectively. We believe that the second value is greater due to the integration error itself, as the relative deviation of ρ has a much sharper maximum in this case (compare Fig. 4). However, both obtained results suggest very good accuracy of the solutions as well as very good quality of the Green's function approximation even for relatively large magnitude of the small parameter ε . Note, that accuracy of the uniform asymptotic formula increase (decrease) with time in case of source (sink).

Next, we consider the inclusion with two degrees of freedom (translations) analysing its movement in two cases. In the first of them, the friction term

in equations (4.35) - (4.36) is neglected. The second variant accounts for the friction phenomenon. We assume in the computations that $\kappa = Q/(4\pi/\epsilon)$ and thus the multipliers in both terms representing forces are the same and equal to $\epsilon Q/(4m)$. In both cases we assume that initial position of the inclusion is $\mathbf{z}_0(0) = 0.1 + 0.1i$ and its initial velocity is zero.

The evolution of the free boundary and the obstacle movement for the frictionless variant are shown in Fig. 5. Starting from zero initial velocity, the obstacle moves rectilinearly along the line: the source - center of the inclusion. We do not present a respective picture for the second variant of the problem, as the free boundary shape is hardly distinguishable from the former. Relative deviations from the benchmark values of $\rho(t_{max}, \theta)$ for both cases are depicted in Fig. 6. The balance equation was satisfied this time to the level of 10^{-8} .

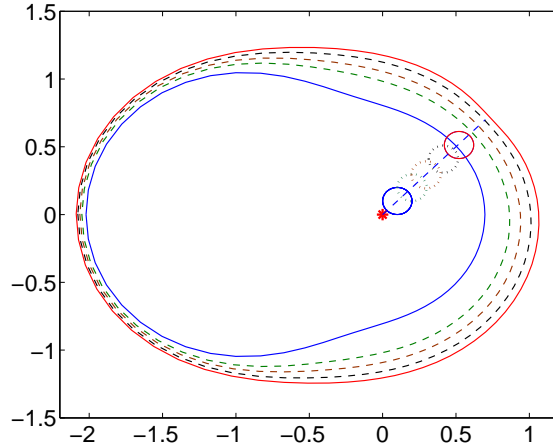


Figure 5: The domain evolution and obstacle movement for the frictionless variant of the problem. Dashed lines illustrate selected intermediate positions.

The influence of friction on the inclusion movement is shown in Fig. 7- Fig. 8. As the obstacle moves in both cases along the straight line, it is sufficient to present the evolution in time of: the covered distance (Fig. 7) - $s(t)$, the absolute value of the velocity (Fig. 8a) - $|\mathbf{v}(t)|$, and the absolute value of the acceleration (Fig. 8b) - $|\mathbf{a}(t)|$.

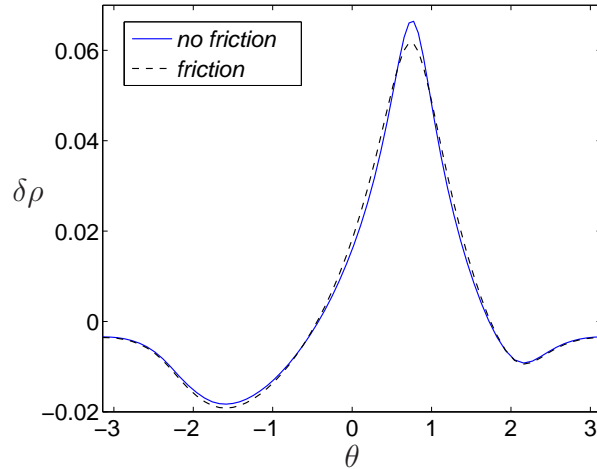


Figure 6: Relative deviations of the radius vector from the benchmark value.

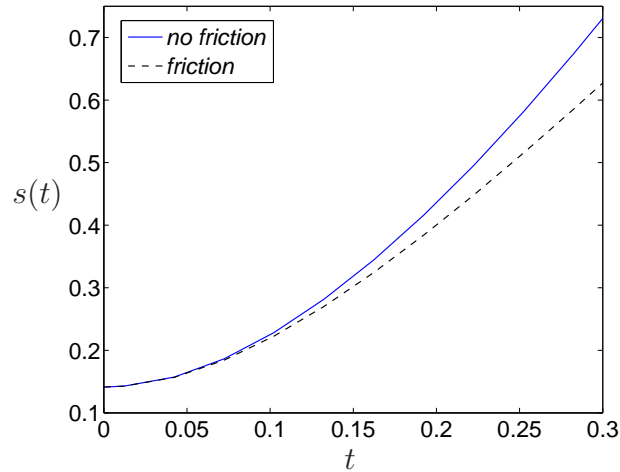


Figure 7: The distance covered by the inclusion.

As anticipated, the influence of friction becomes more pronounced along with the velocity increase, however in the considered time interval it is still far away from making the inclusion movement uniform. Obviously by increasing the value of friction coefficient one can obtain the steady state much faster.

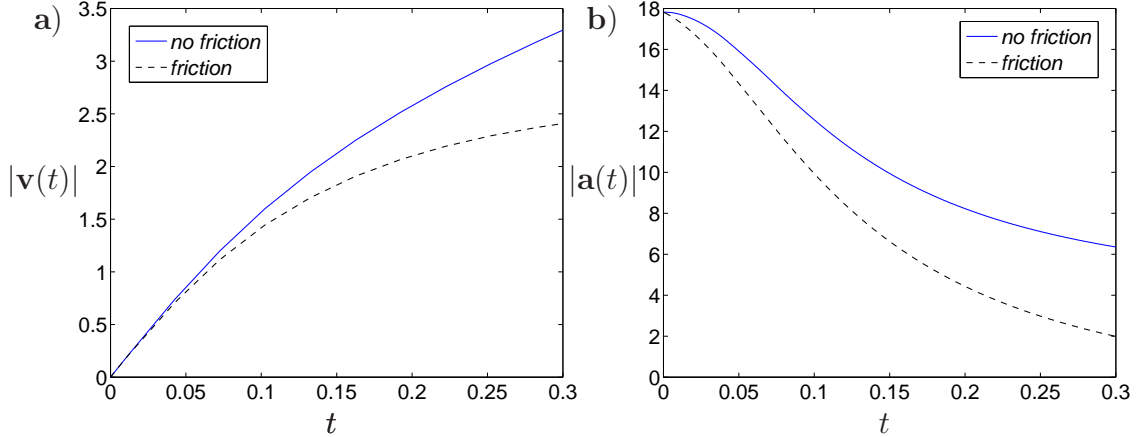


Figure 8: The absolute values of: a) the inclusion velocity, b) the inclusion acceleration.

In the last part of our analysis we consider the case when the initial velocity of the inclusion has a non-zero value, and its vector is not collinear with the line: center of inclusion - source. We investigate the evolution of obstacle track, velocity and acceleration caused by the fluid flow. It is assumed that the initial position of the obstacle is $\mathbf{z}_0(0) = -0.5 - 0.5i$, while its initial velocity yields $\mathbf{v}(0) = 2i$. We consider two variants of the problem depicted in Fig. 9. In the first one, the fluid flow is driven by the source and initial shape of the free boundary is described by the internal curve. The second variant assumes the domain contraction caused by the fluid sink. Here, the initial domain is defined by the external curve. This time we shall rather concentrate on the inclusion movement, than on the evolution of the free boundary. The relative deviations of the radius vector from respective reference (benchmark) values are shown in Fig. 10. Naturally, the variant with the sink gives more pronounced deformation of the final shape, as the distance between the inclusion and the boundary is much smaller than in the opposite case. The fluid balance equation was satisfied to the level of 10^{-8} for the variant of domain expansion, and 10^{-7} for domain contraction.

The traces of inclusion for both considered cases are shown by markers in Fig. 9. It should be emphasized that the imposed initial conditions do not imply kinematic equivalence between both variants of the problem. It is a consequence of different initial accelerations resulting from equations (4.35) -

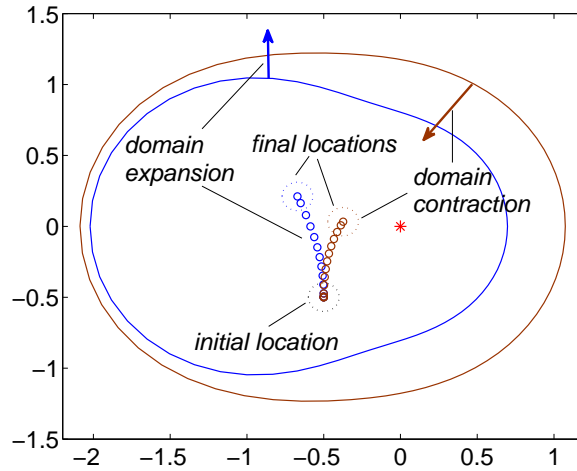


Figure 9: Domain configuration and obstacle movement. Markers correspond to intermediate positions of the inclusion. Depicted boundary curves define the initial shapes of the domain for respective variants of the problem.

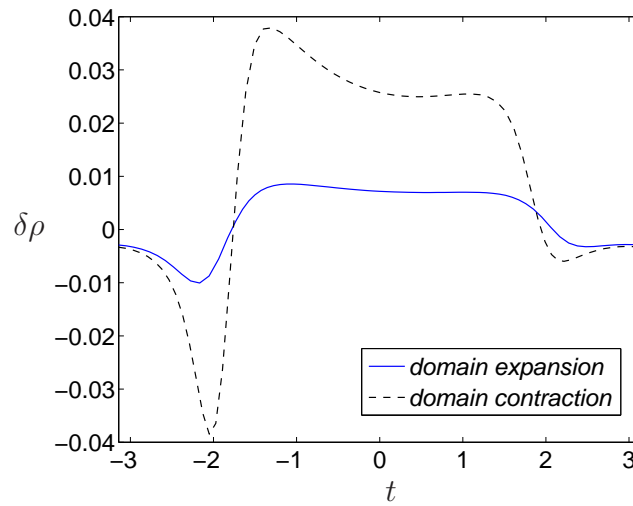


Figure 10: Relative deviations of the radius vector from the benchmark values (without inclusion).

(4.36). As can be seen in Fig. 12, Fig. 14, although the magnitudes of initial accelerations are very close to each other, their vectors directions are almost opposite.

The curvatures of the tracks (bend directions) and the signs of respective components of acceleration are determined by the source/sink activity. In the case of domain expansion the fluid flow direction magnifies the velocity of obstacle. Thus the distance covered is greater than that for fluid sink. Obviously, for other configurations of the initial velocity vector one can expect different trends.

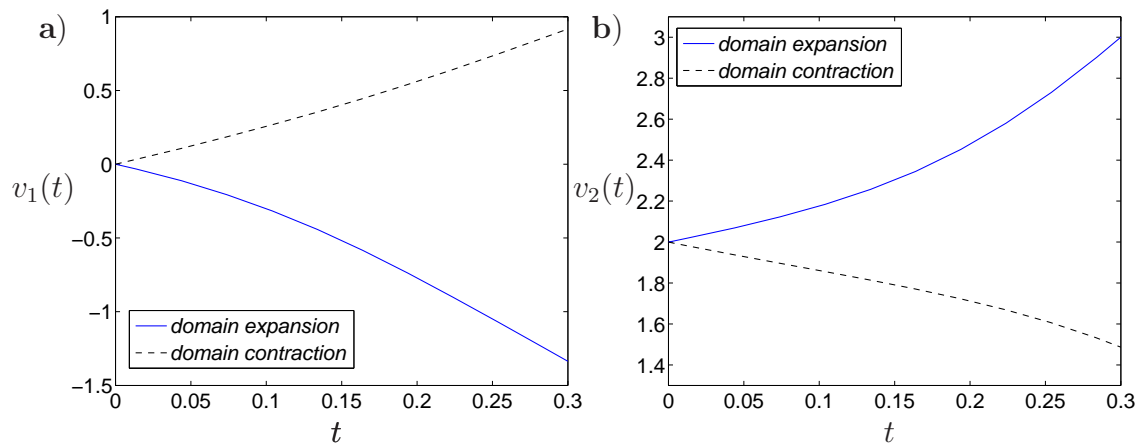


Figure 11: Components of the inclusion velocity: a) horizontal, b) vertical.

Concluding this section, we have shown that the method utilized the uniform asymptotic expansion for the Green function delivered in [25] is effective and the computations based on that approach are stable and robust.

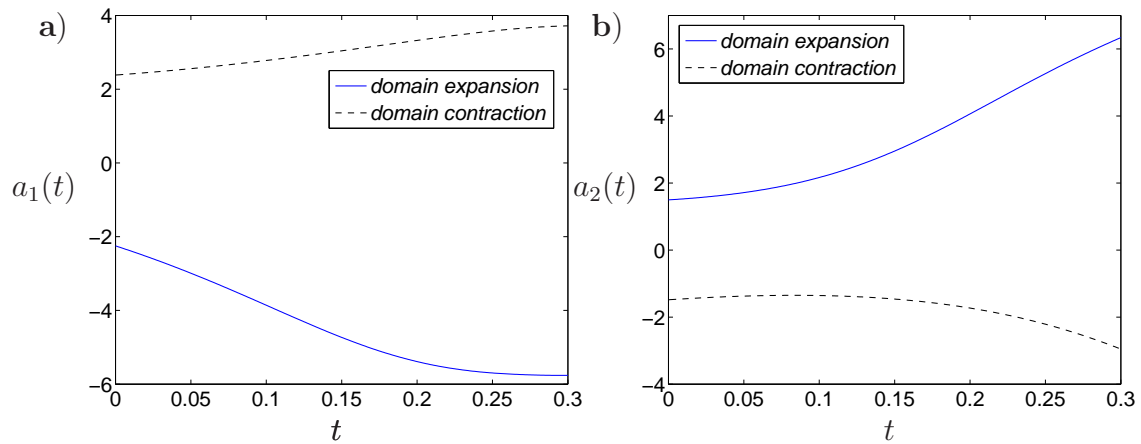


Figure 12: Components of the inclusion acceleration: a) horizontal, b) vertical.

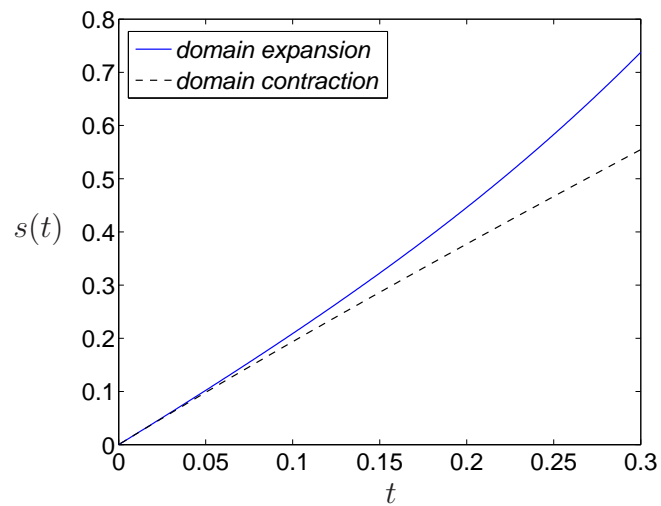


Figure 13: The distance covered by the inclusion.

Acknowledgement. The work has been supported by PEOPLE IAPP Project PIAP-GA-2009-251475 HYDROFRAC.

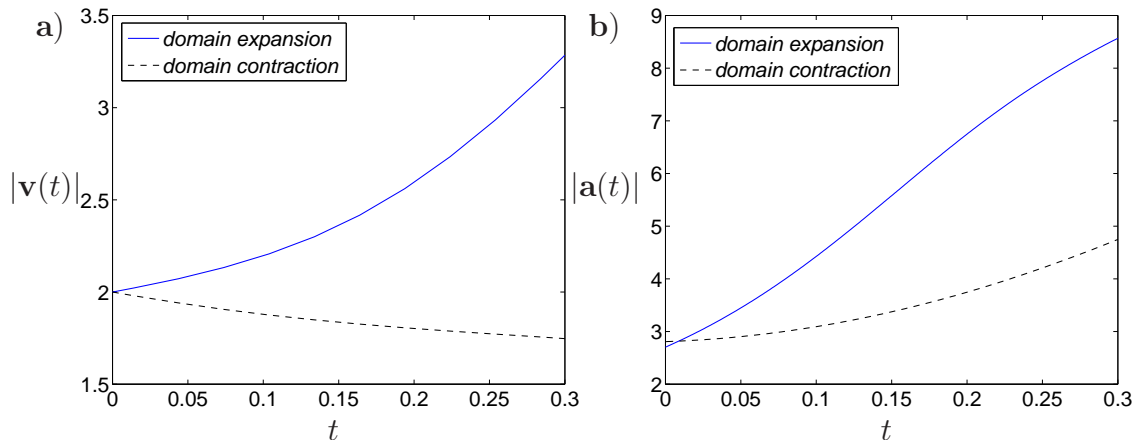


Figure 14: The absolute values of: a) inclusion velocity, b) inclusion acceleration.

References

- [1] S.N. Antontsev, C.R. Gonçalves, A.M. Meirmanov, Local existence of classical solutions to the well-posed Hele-Shaw problem, *Port. Math. (N.S.)*, **59**, No. 4, 2002, 435–452.
- [2] S.N. Antontsev, C.R. Gonçalves, A.M. Meirmanov, Exact estimates for the classical solutions to the free-boundary problem in the Hele-Shaw cell. *Adv. Differ. Equ.* **8**, No. 10, 2003, 1259–1280.
- [3] S.N. Antontsev, A.M. Meirmanov, B.V. Yurinsky, Weak solutions for a well-posed Hele-Shaw problem. *Boll. Unione Mat. Ital., Sez. B, Artic. Ric. Mat.*, (**8**) **7**, No. 2, 2004, 397–424.
- [4] H. Begehr, R.P. Gilbert, Hele-Shaw type flows in \mathbb{R}^n , *Nonlinear Analysis*, **10**, 1986, 65–85.
- [5] M. C. Dallaston, S. W. McCue, New exact solutions for Hele-Shaw flow in doubly connected regions, *Physics of Fluids*, **24**, 2012, 052101.
- [6] T. A. Driscoll, Algorithm 756: A MATLAB Toolbox for Schwarz-Christoffel mapping, *ACM Trans. Math. Soft.*, **22**, 1996, 168–186.

- [7] T. A. Driscoll, Algorithm 843: Improvements to the Schwarz–Christoffel toolbox for MATLAB. *ACM Trans. Math. Soft.*, **31**, 2005, 239–251.
- [8] V. Entov, P. Etingof, On the break of air bubbles in a Hele-Shaw cell, *Eur. J. Appl. Math.*, **22**, No. 2, 2011, 125–149.
- [9] J. Escher, G. Simonett, Maximal regularity for a free boundary problem, *Nonlinear Differential Equations Appl.*, **2**, 1995, 463–510.
- [10] J. Escher, G. Simonett, Classical solutions of multidimensional Hele-Shaw models, *SIAM J. Math. Anal.*, **28**, No. 5, 1997, 1028–1047.
- [11] L.A. Galin, Unsteady filtration with a free surface, *Dokl. Akad. Nauk USSR*, **47**, 1945, 246–249. (in Russian)
- [12] D. Gilbarg, N.S. Trudinger, *Elliptic Partial Differential Equations of Second Order*, 2nd ed., Springer, Berlin, 2001.
- [13] I. S. Gradshteyn, I. M. Ryzhik, *Table of Integrals, Series, and Products*, Academic Press, Amsterdam-Boston etc., 2007 (7th edition).
- [14] B. Gustafsson, On a differential equation arising in a Hele-Shaw flow moving boundary problem, *Arkiv för matematik*, **22**, 1984, 251–268.
- [15] B. Gustafsson, Applications of variational inequality approach to the moving boundary problem for Hele-Shaw flows, *SIAM J. Math. Anal.*, **16**, No. 2, 1985, 279–300.
- [16] B. Gustafsson, A. Vasil'ev, *Conformal and Potential Analysis in Hele-Shaw cells*, Birkhäuser Verlag, Basel-Boston-Berlin, 2006.
- [17] J. Hadamard, Sur le problème d'analyse relatif à l'équilibre des plaques élastiques encastrées. *Memoire couronne en 1907 par l'Académie des Sciences*, **33**, No. 4, 1907, 515–629.
- [18] H. S. Hele-Shaw, The flow of water, *Nature*. **58(1489)**, 1898, 33–36.
- [19] Yu.E. Hohlov, M. Reissig, On classical solvability for the Hele-Shaw moving boundary problem with kinetic undercooling regularization, *Euro. J. Applied Math.*, **6**, 1995, 421–439.

- [20] S. D. Howison, Complex variable methods in Hele-Shaw moving boundary problems. *Euro. J. Appl. Math.*, **3**, 1992, 209–224.
- [21] P. P. Kufarev, Yu. P. Vinogradov, On a filtration problem. *Prikl. Mat. Mech.* **12**, 1948, 181–198 (in Russian) (English translation: University of Delaware, Applied Mathematics Institute, Technical Report 182A, 1984).
- [22] V. Maz'ya, A. Movchan, Uniform asymptotics of Green's kernels for mixed and Neumann problems in domains with small holes and inclusions. Isakov, Victor (ed.), *Sobolev spaces in mathematics. III: Applications in mathematical physics*. New York, NY: Springer; Novosibirsk: Tamara Rozhkovskaya Publisher. International Mathematical Series **10**, 2009, 277–316.
- [23] V. Maz'ya, A. Movchan, Uniform asymptotics of Green's kernels in perforated domains and meso-scale approximation, *Complex Variables and Elliptic Equations*, **57**, No. 2, 2012. 137–154.
- [24] V. Maz'ya, A. Movchan, M. Nieves, Uniform asymptotic formulae for Green's tensors in elastic singularly perturbed domains with multiple inclusions. *Rendiconti. Accademia Nazionale delle Scienze detta dei XL, Memorie di Matematica e Applicazioni*, 124^o, Vol. **XXX**, 2006, 103–158.
- [25] V. Maz'ya, A. Movchan, M. Nieves, *Green's Kernel and Meso-Scale Approximations in Perforated Domains*. Lecture Notes in Mathematics, **2077**, Springer, Heidelberg etc., 2013.
- [26] G. Mishuris, S. Rogosin, M. Wrobel, Hele-Shaw Flow with a small obstacle. *Meccanica* (in print).
- [27] L. Nirenberg, An abstract form of the nonlinear Cauchy-Kowalevski theorem, *J. Differential Geom.*, **6**, 1972, 561–576.
- [28] T. Nishida, A note on a theorem of Nirenberg, *J. Differential Geom.*, **12**, 1977, 629–633.
- [29] L. V. Ovsjannikov, A singular operator in a scale of Banach spaces, *Dokl. AN SSSR*, **163**, No. 4, 1965, 819–822 (in Russian).

- [30] N. Papamichael, *Lectures on Numerical Conformal Mapping*, University of Cyprus, 2008.
- [31] P. Ya. Polubarinova-Kochina, On the motion of the oil contour, *Dokl. Akad. Nauk SSSR*, **47**, 1945, 254–257 (in Russian).
- [32] M. Reissig, About a nonstationary mixed problem for holomorphic functions arising by the study of a potential flow past a circular cylinder with permeable surface, *Math. Nachr.*, **164**, 1993, 283–297.
- [33] M. Reissig, L. von Wolfersdorf, A simplified proof for a moving boundary problem for Hele-Shaw flows in the plane, *Arkiv för Math.*, **31**, No. 1, 1993, 101–110.
- [34] M. Reissig, The existence and uniqueness of analytic solutions for moving boundary value problem for Hele-Shaw flows in the plane, *Nonlinear Anal. Theory, Methods & Appl.*, **23**, No. 5, 1994, 565–576.
- [35] M. Reissig and S.V. Rogosin, with an appendix of F. Huebner, Analytical and numerical treatment of a complex model for Hele-Shaw moving boundary value problems with kinetic undercooling regularization, *Euro J. Appl. Math.*, **10**, 1999, 561–579.
- [36] S .D. Richardson, Hele-Shaw flows with a free boundary produced by injection of fluid into a narrow channel. *J. Fluid Mech.*, **56**, 1972, 609–618.
- [37] A. Vasil’ev, From the Hele-Shaw experiment to integrable systems: a historical overview, *Compl. Anal. Oper. Theory*, **3**, 2009, 551–585.